

Determination of the safe working zone of a parallel manipulator

Rangaprasad Arun Srivatsan and Sandipan Bandyopadhyay

Abstract This paper formalises the concept of *safe working zone* (SWZ) of a parallel manipulator, which is a subspace of the workspace that is free of singularities as well as issues of joint limits and link interference. It presents further a generic scheme to identify such a space, and specialises the same for the case of a convex SWZ around a chosen point of interest. The theoretical developments are illustrated via an application on a three-degree-of-freedom spatial parallel manipulator, namely, MaPaMan-I.

Key words: Parallel manipulator, workspace, singularities, link interference, joint limits.

1 Introduction

Parallel manipulators (PMs) offer better load-carrying capacity and accuracy than their serial counterparts. Still, they are not as popular as the latter in the industries. This may be attributed mainly to the complicated kinematics of PMs, which in turn lead to small workspace volumes, rendered even smaller by the existence of *gain-type* singularities inside the workspace. In addition, joint limits and link interference further reduce the usable workspace.

Researchers have attempted to alleviate these problems in different ways. Some have attempted to design the robot such that the singularities are excluded [9, 13]. Others have tried to find regions inside the workspace that are free of singularities [3, 8]. The latter approach requires algebraic operations on the analytical description of the singular manifold, which is very difficult

Rangaprasad Arun Srivatsan e-mail: rarunsrivatsan@gmail.com
Sandipan Bandyopadhyay
Department of Engineering Design, Indian Institute of Technology Madras,
Chennai - 600036, India. e-mail: sandipan@iitm.ac.in

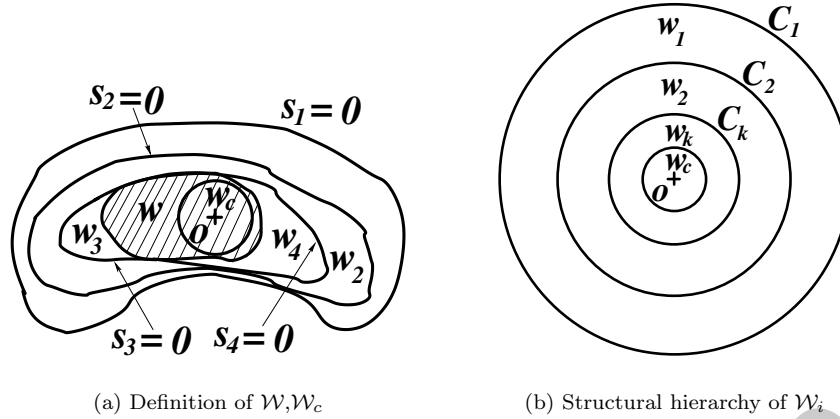


Fig. 1 Definition and structure of \mathcal{W} and \mathcal{W}_c

in general, and may not be possible for all manipulators. This has motivated the development of some numerical schemes to find singularity-free zones inside the workspace [6, 2]. In [4, 11, 5], additional kinematic constraints, i.e., joint limits and link interference, have been considered.

The ultimate objective of all of these, and similar works, is to *identify a subset of the workspace, in which the manipulator can move freely*. This would render the task of path planning trivial, so long as the manipulator stayed inside the said space – which is very attractive from the point of view of applications. In this paper, such a space has been defined as the *safe working zone* (SWZ) of a PM. The criteria for the determination of the same, while considering the singularities, kinematic constraints etc. have been laid down clearly, which in turn have been used to develop a computational framework to compute the SWZ. The theoretical development is then illustrated by means of application to a newly introduced PM, namely, MaPaMan-I [12]. The scheme can be applied to any other PM, or even a serial manipulator.

The rest of the paper is organised in the following manner: in Section 2, the concept of SWZ is formalised. Various boundary functions specific to MaPaMan-1 are presented in Section 3, followed by the numerical results in Section 4. Finally the conclusions are presented in Section 5.

2 Definition and structure of the SWZ

Various terms, such as *practical/desired/specific* workspace have been used in literature to designate subsets of the workspace, which are either free of

singularities, kinematic constraints, or both (see, e.g., [10, 4]). Such confusion necessitates the formalisation of the definition of the SWZ.

Definition 1. The SWZ of a manipulator (denoted by \mathcal{W}) is defined as the subset of the workspace of the manipulator satisfying the following criteria:

1. \mathcal{W} is contained *inside* the workspace, i.e., it is free of loss-type singularities.
2. \mathcal{W} does not contain or touch the singular manifold, i.e., \mathcal{W} is free of gain-type singularities as well.
3. At no point of \mathcal{W} there is an interference between the links, even when the actual physical dimensions of the links are considered.
4. At no point of \mathcal{W} does any joint violate a physical limit on its range of motion. Once again, the actual physical dimensions are to be considered.
5. \mathcal{W} is a *connected* set, containing a given point of interest, ' \mathbf{o} '.

The requirements 1-4 each define a subset of the workspace, which is bounded by the *zero level-set* of a corresponding function:

- The workspace (denoted by \mathcal{W}_1), is bounded by the loss-type singularity condition, given by $S_1 = 0$.
- The region \mathcal{W}_2 containing \mathbf{o} and free of gain-type singularities, is bounded by the set of points defining the singular manifold which satisfy $S_2 = 0$.
- The region that includes \mathbf{o} and is free of link interference is denoted by \mathcal{W}_3 , and is bounded by the set satisfying $S_3 = 0$.
- The set of points satisfying $S_4 = 0$ bounds \mathcal{W}_4 , the space containing \mathbf{o} that is free of joint-limit violations.

As seen in Fig. 1(a), $\mathcal{W} = \bigcup_{i=1}^4 \mathcal{W}_i$ ¹. Note that in Fig. 1(b), \mathcal{W}_k could be \mathcal{W}_3 or \mathcal{W}_4 , or both. Physical considerations impose the following hierarchy: $\mathcal{W} \subset \mathcal{W}_3 \cup \mathcal{W}_4 \subset \mathcal{W}_2 \subset \mathcal{W}_1$. Moreover, it is generally preferred to identify a *convex set* $\mathcal{W}_c \subset \mathcal{W}$. These observations motivate a scheme for the computation of the final result, namely, \mathcal{W}_c . The steps are described below.

1. Compute \mathcal{W}_1 . Find its *largest* convex subset, \mathcal{W}_{c_1} , centred at \mathbf{o} . The region can be in the form of convex polyhedra, super-ellipsoids, ellipsoids, etc. Without any loss of generality, and for the ease of computation, in this work *circles* have been used in the 2-dimensional subsets of the workspace (see Section 4). As shown in Fig. 1(b), the circle C_1 bounds \mathcal{W}_{c_1} .
2. In a similar manner, find C_2 , which bounds \mathcal{W}_{c_2} . Obviously, $\mathcal{W}_{c_2} \subset \mathcal{W}_{c_1}$.
3. Compute the corresponding entities, namely, $\mathcal{W}_{c_3}, C_3, \mathcal{W}_{c_4}, C_4$ accordingly. Finally, find $\mathcal{W}_c = \mathcal{W}_{c_3} \cup \mathcal{W}_{c_4} \subset \mathcal{W}_{c_2}$.

The above steps are obvious, as it is useless to consider points *outside* \mathcal{W}_{c_1} while computing \mathcal{W}_{c_2} , and so on. However, the implication of the hierarchy is very significant in the actual implementation of the scheme. Due to the lack/complexity of analytical results, most often, the set boundaries

¹ Note that not all manipulators have all the four requirements. In all serial manipulators, $\mathcal{W}_1 = \mathcal{W}_2$, and as explained in Section 3, for MaPaMan-I, $\mathcal{W}_3 = \mathcal{W}_4$.

mentioned above need to be computed through numerical searches (see, e.g., [7, 10, 4, 2, 11]), and hence the progressively diminishing domain for the search algorithm helps reducing the computational requirements for a given desired level of resolution of the results obtained.

3 Formulation of the SWZ of MaPaMan-I

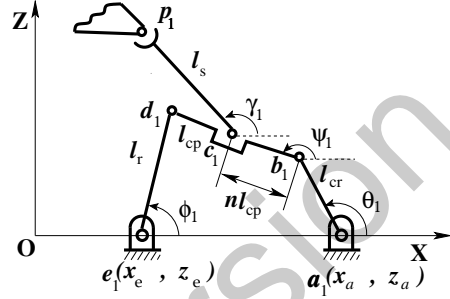


Fig. 2 Prototype (left) and kinematic details of a leg (right) of MaPaMan-I

The generic theoretical framework described in Section 2 is illustrated in this section by an application to the newly developed MaPaMan-I. It so happens that for the physical dimensions of the present prototype described in [12], the joints have limits on their motions, but there is no other form of link interference. Thus, the computation of \mathcal{W}_3 (or, \mathcal{W}_{c_3}) is not required.

MaPaMan-I has 3-degrees-of-freedom similar to 3-RPS and its task-space can be parametrised in terms of roll (α), pitch (β) and heave (z_c) [12]. The coordinates of the end-effector \mathbf{p}_i ($i = 1, 2, 3$) are obtained from the task-space coordinates $\mathbf{x} = (\alpha, \beta, z_c)^T$. The input joint angles are: $\boldsymbol{\theta} = (\theta_1, \theta_2, \theta_3)^T$, and the passive joint angles are: $\boldsymbol{\phi}, \boldsymbol{\psi}$ and $\boldsymbol{\gamma}$ (see Fig. 2).

3.1 Condition for loss-type singularity (S_1)

Following [14], kinematic constraints are first framed to relate the task-space coordinates to the input coordinates. The length of the strut, l_s , is fixed, hence the *loop-closure* constraints can be cast as: $f_i(\theta_i, \psi_i, \mathbf{x}) \triangleq \|\mathbf{b}_i - \mathbf{p}_i\| = l_s$, $i = 1, 2, 3$. Likewise, the loop-closure equations for the four-bars (see Fig. 2), upon elimination of the passive variable ϕ_i , become [12]: $g_i(\theta_i, \psi_i) = l_0^2 + l_{cr}^2 + l_{cp}^2 - l_r^2 + 2l_0l_{cr} \cos \theta_i + 2l_0l_{cp} \cos \psi_i + 2l_{cr}l_{cp} \cos \theta_i \cos \psi_i + 2l_{cr}l_{cp} \sin \theta_i \sin \psi_i$. From each pair of f_i and g_i , the passive variable ψ_i is eliminated to ob-

tain $h_i(\theta_i, \mathbf{x}) = 0$, $i = 1, 2, 3$. The condition for loss type singularity is given by $S_1 = 0$, where $S_1 = \det\left(\frac{\partial \mathbf{h}}{\partial \boldsymbol{\theta}}\right)$, and $\mathbf{h} = (h_1(\theta_1, \mathbf{x}), h_2(\theta_2, \mathbf{x}), h_3(\theta_3, \mathbf{x}))^T$.

3.2 Condition for gain-type singularity (S_2)

Following [12], the loop-closure constraints are cast in the form $\boldsymbol{\eta}(\boldsymbol{\theta}, \boldsymbol{\psi}, \boldsymbol{\gamma}) = \mathbf{0}$, which upon time-differentiation yield $\dot{\boldsymbol{\eta}}(\mathbf{q}) = \mathbf{J}_{\boldsymbol{\eta}\boldsymbol{\theta}}\dot{\boldsymbol{\theta}} + \mathbf{J}_{\boldsymbol{\eta}\boldsymbol{\psi}}\dot{\boldsymbol{\psi}} + \mathbf{J}_{\boldsymbol{\eta}\boldsymbol{\gamma}}\dot{\boldsymbol{\gamma}}$, where $\mathbf{J}_{\boldsymbol{\eta}\boldsymbol{\theta}} = \frac{\partial \boldsymbol{\eta}}{\partial \boldsymbol{\theta}}$, $\mathbf{J}_{\boldsymbol{\eta}\boldsymbol{\psi}} = \frac{\partial \boldsymbol{\eta}}{\partial \boldsymbol{\psi}}$, and $\mathbf{J}_{\boldsymbol{\eta}\boldsymbol{\gamma}} = \frac{\partial \boldsymbol{\eta}}{\partial \boldsymbol{\gamma}}$. Considering the four-bar alone, $\dot{\boldsymbol{\psi}} = \mathbf{J}_{\boldsymbol{\psi}\boldsymbol{\theta}}\dot{\boldsymbol{\theta}}$, where $\mathbf{J}_{\boldsymbol{\psi}\boldsymbol{\theta}}$ is always well-defined, since by design, the said four-bars satisfy Grashoff's condition. Therefore, $(\mathbf{J}_{\boldsymbol{\eta}\boldsymbol{\theta}} + \mathbf{J}_{\boldsymbol{\eta}\boldsymbol{\psi}}\mathbf{J}_{\boldsymbol{\psi}\boldsymbol{\theta}})\dot{\boldsymbol{\theta}} + \mathbf{J}_{\boldsymbol{\eta}\boldsymbol{\gamma}}\dot{\boldsymbol{\gamma}} = \mathbf{0}$. The gain-type singularity occurs when the *passive velocity*, $\dot{\boldsymbol{\gamma}}$, cannot be found uniquely for a given $\dot{\boldsymbol{\theta}}$ [1]. This leads $S_2 = 0$, where $S_2 = \det(\mathbf{J}_{\boldsymbol{\eta}\boldsymbol{\gamma}})$.

3.3 Condition for the violation of joint limits (S_4)

The issue of the joints reaching their limits in the range of motion is observed at the cranks, the strut-coupler rotary joints, and the spherical joints attached to the end-effector. The following are various limiting conditions for the same:

- The crank is designed such that it is always above the base of the manipulator. From practical considerations, a restriction is imposed upon the maximum and the minimum angle of rotation of the crank denoted by θ_{min} , and θ_{max} , respectively (see Fig. 3(a)). Thus, $0 < \theta_i < \theta_{max}$, $i = 1, 2, 3$. Hence the conditions defining the boundary of unacceptable points are $s_{1i} = 0$ and $s_{2i} = 0$, where $s_{1i} = \theta_i - \theta_{min}$, $s_{2i} = \theta_{max} - \theta_i$.
- The angle made by the strut relative to the coupler is limited by the physical joint limits as shown in Fig. 3(b), denoted by γ_{min} and γ_{max} , where $\gamma_{min} < (\pi + \gamma_i - \psi_i) < \gamma_{max}$, $i = 1, 2, 3$. Thus the conditions defining the boundary of the unacceptable sets are: $s_{3i} = 0$, and $s_{4i} = 0$; where $s_{3i} = (\pi + \gamma_i - \psi_i) - \gamma_{min}$, $s_{4i} = \gamma_{max} - (\pi + \gamma_i - \psi_i)$.
- The spherical joints have restricted motions due to the physical dimensions of their constituent mechanical components. This can be modelled as a limit imposed on the angle δ_i , such as $0 < \delta_i < \delta_{max}$ (see Fig. 3(c)). The angle δ_i is computed by first finding a vector along the direction of strut (\mathbf{v}_1) and then measuring the angle between it and the normal (\mathbf{n}) to the end-effector: $\mathbf{v}_1 = (\mathbf{b}_1 - \mathbf{p}_1)/l_s$, $\mathbf{n} = (\mathbf{p}_1 - \mathbf{p}_2) \times (\mathbf{p}_3 - \mathbf{p}_1)/\frac{\sqrt{3}d_1^2}{2}$ and $\delta_1 = \arccos(\mathbf{n} \cdot \mathbf{v}_1)$. Similarly, δ_2 and δ_3 are computed. Therefore the functions defining the boundary of the desirable set are given by $s_{5i} = 0$, where $s_{5i} = \delta_{max} - \delta_i$. The function S_4 is obtained from the product of individual functions: $S_4 = \prod s_{ij}$, where $i = 1, \dots, 5$, and $j = 1, 2, 3$.

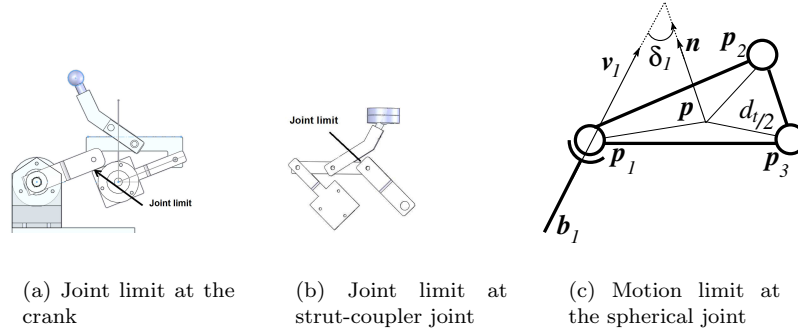


Fig. 3 Joint limits imposed by the physical dimensions of MaPaMan-I

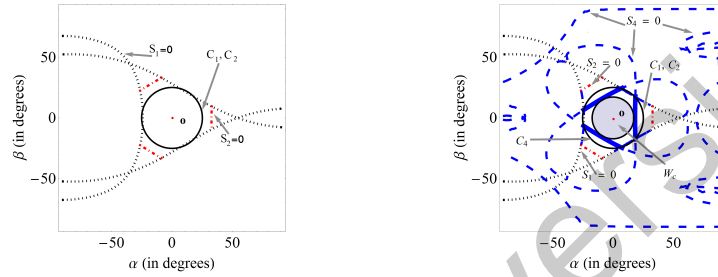


Fig. 4 Zero level-sets of S_i , and C_i in the α - β slice of the workspace at $z_c = 135\text{mm}$

4 Numerical results

This section describes the results of the application of the above formulation to the MaPaMan-I prototype, whose dimensions are given in Table 1 of [12]. The joint limits used are: $\theta_{min} = 25^\circ$, $\theta_{max} = 90^\circ$, $\gamma_{min} = 0^\circ$, $\gamma_{max} = 120^\circ$, $\delta_{max} = 60^\circ$. The task-space of MaPaMan-I is parametrised by (α, β, z_c) . The functions S_i are not available solely in terms of these variables. Therefore instead of direct computation of the zero level-sets, these are found by using a numerical scheme similar to those used in [4, 2]. Since it is computationally demanding to search for solutions of $S_i = 0$ in a 3-dimensional space, 2-dimensional slices in roll and pitch are considered instead, and the solutions are evaluated in these slices for a sequence of heave values². Fig. 4 shows the zero level-sets of S_1, S_2 in the α - β plane obtained by slicing the workspace at $z_c = 135\text{mm}$. Note that the points satisfying $S_2 = 0$ fall outside \mathcal{W}_{c_1} , and therefore in this particular case, $C_2 = C_1$. The zero level-set of $S_4 = 0$ is shown in the entire scan range in Fig. 4. However, only the parts of it

² Zero level-sets of S_1, S_2, S_4 have been computed using ContourPlot in Mathematica.

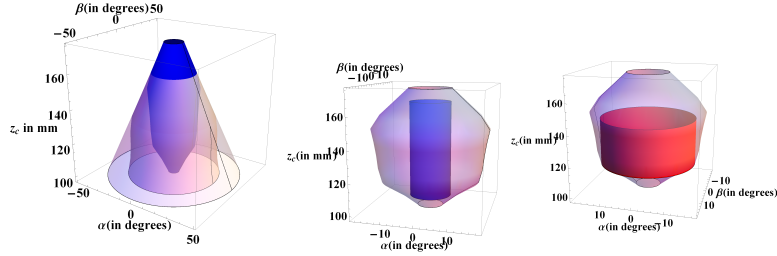


Fig. 5 Left: Stack of C_1 , C_2 , C_4 in MaPaMan-I, Middle: \mathcal{W}_c as a cylinder for $z_c \in (98.4, 166.5)$ mm, Right: \mathcal{W}_c as a cylinder for $z_c \in (111.3, 145.2)$ mm

appearing inside \mathcal{W}_{c_2} (marked by thicker lines in Fig. 4) are considered for the computation of \mathcal{W}_{c_4} . As noted earlier, in this case, $\mathcal{W}_c = \mathcal{W}_{c_4}$. Naturally, the stack of C_4 obtained for all the slices when put together yields a subset of \mathcal{W} , that is convex in each slice. This does not necessarily imply that the stack delimits a convex region as a whole. However, one can easily fit a desired convex shape to obtain \mathcal{W}_c in the (α, β, z_c) space. Due to the nature of the degree-of-freedom of the manipulator, a cylinder is chosen as the convex shape to be fit inside \mathcal{W} . Fig. 5 shows the stack of C_1 , C_2 and C_4 together for the manipulator under consideration. Note how they follow the hierarchy described in Section 2. As the stack of C_4 has been obtained for the entire range of heave, \mathcal{W}_c can be obtained by fitting a convex shape to the stack for any desired subset of the complete range of heave. Note that the radius of the cylinder in the former case is 6.59° while it is 15.62° in the latter (see Fig. 5). Thus, based on the intended application, a convex shape of interest can be fit into \mathcal{W} to obtain \mathcal{W}_c desired.

5 Conclusion

In this paper, the concept of a safe working zone of a parallel manipulator has been formalised, and a generic framework has been presented for its computation. It has been shown that considering a convex subset of the same can lead to a hierarchy in the subsets leading to the final result, reducing the computational requirements significantly in the process. The formulation has been demonstrated by means of an application on a newly developed parallel manipulator, namely MaPaMan-I, whose workspace and singularities were not reported previously. A single computational tool, namely a contour-plotter in a 2-dimensional space, has been used to compute the SWZ and its convex subsets. The generic and simple nature of the scheme presented in this paper can help in identifying the SWZ in similar manipulators, as well as be used in the design of manipulators for a desired SWZ.

References

- [1] Bandyopadhyay, S., Ghosal, A.: Analytical determination of principal twists in serial, parallel and hybrid manipulators using dual number algebra. *Mechanism and Machine Theory* **39**(12), 1289–1305 (2004)
- [2] Bohigas, O., Zlatanov, D., Ros, L., Manubens, M., Porta, J.: Numerical computation of manipulator singularities. In: *Proceedings of the 2012 ICRA*, pp. 1351–1358 (2012)
- [3] Bonev, I.A., Gosselin, C.M.: Singularity loci of planar parallel manipulators with revolute joints. In: *Proceedings of the 2nd Workshop on Computational Kinematics*, pp. 291–299. Seoul, South Korea (2001)
- [4] Cao, Y., Huang, Z., Zhang, Q., Zhou, H., Ding: Orientation-workspace analysis of the Stewart-Gough manipulator. In: *Proceedings of the ASME DETC 2005/MECH-84556*. California, USA (2005)
- [5] Chablat, D., Wenger, P.: Moveability and collision analysis for fully-parallel manipulators. *Computing Research Repository* **0707.1957v1** (2007)
- [6] Huag, E., Luh, C.M., Adkins, F.A., Wang, J.Y.: Numerical algorithms for mapping boundaries of manipulator workspaces. *Journal of Mechanical Design* **118**(2), 228–234 (1996)
- [7] Hudgens, J., Arai, T.: Planning link-interference-free trajectories for a parallel link manipulator. In: *Proceedings of the IECON '93*, vol. 3, pp. 1506–1511 (1993)
- [8] Jiang, Q., Gosselin, C.M.: The maximal singularity-free workspace of the Gough-Stewart platform for a given orientation. *Journal of Mechanical Design* **130**(11) (2008)
- [9] Liu, X.J., Wang, J.S., Gao, F.: On the optimum design of planar 3-dof parallel manipulators with respect to the workspace. In: *Proceedings of the 2000 ICRA*, vol. 4, pp. 4122–4127 (2000)
- [10] Merlet, J.P.: Designing a parallel manipulator for a specific workspace. *International Journal of Robotics Research* **16**(4), 545–556 (1997)
- [11] Pernkopf, F., Husty, M.L.: Workspace analysis of Stewart-Gough-type parallel manipulators. *Journal of Mechanical Engineering Science* **220**(7), 1019–1032 (2006)
- [12] Srivatsan, R.A., Bandyopadhyay, S.: On the position kinematic analysis of MaPaMan: A reconfigurable three-degrees-of-freedom spatial parallel manipulator. *Mechanism and Machine Theory* **62**(4), 150–165 (2013)
- [13] Yang, Y., O'Brien, J.: A geometric approach for the design of singularity-free parallel robots. In: *Proceedings of the 2009 ICRA*, pp. 1801–1806. Kobe, Japan (2009)
- [14] Zlatanov, D., Bonev, I.A., Gosselin, C.M.: Constraint singularities of parallel mechanisms. In: *Proceedings of the 2002 ICRA*, pp. 496–502. Washington DC, USA (2002)